*Earth Planets Space*, **65**, 591–607, 2013

# Precursory activity and evolution of the 2011 eruption of Shinmoe-dake in Kirishima volcano—insights from ash samples

Yuki Suzuki[1], Masashi Nagai[2], Fukashi Maeno[1], Atsushi Yasuda[1], Natsumi Hokanishi[1], Taketo Shimano[3], Mie Ichihara[1], Takayuki Kaneko[1], and Setsuya Nakada[1]

[1]*Earthquake Research Institute, University of Tokyo, 1-1-1, Yayoi, Bunkyo-ku, Tokyo 113-0032, Japan*
[2]*National Research Institute for Earth Science and Disaster Prevention, 3-1, Tennodai, Tsukuba, Ibaraki 305-0006, Japan*
[3]*Graduate School of Environment and Disaster Research, Fuji Tokoha University, 325, Obuchi, Fuji, Shizuoka 417-0801, Japan*

(Received October 30, 2012; Revised February 13, 2013; Accepted February 17, 2013; Online published July 8, 2013)

After a precursory phreatic stage (2008 to 2010), the 2011 Shinmoe-dake eruption entered a phreatomagmatic stage on January 19, a sub-Plinian and lava accumulation stage at the end of January, a vulcanian stage in February–April, and a second phreatomagmatic stage in June–August. Component ratio, bulk composition, and particle size of the samples helped us define the eruptive stages. The juvenile particles were first found in the January 19 sample as pumice (8 vol%) and were consistently present as scoria and pumice particles thereafter (generally ∼50 vol%, decreasing in weaker events). The January 19 pumice has water-quench texture. After the lava accumulation, particles of that lava origin came to account for 30∼70 vol% of the ash. The second phreatomagmatic stage is proposed because of fine ash and long eruption period. The $SiO_2$ contents of bulk ash are lower in post-January 19, 2011 eruptions, reflecting lower average $SiO_2$ contents in 2011 ejecta than in past ejecta. The free-crystal assemblages were two pyroxenes + plagioclase + Fe-Ti oxides until 2010; olivine joined the assemblage in 2011, when juvenile ash was erupted. This change is consistent with the absence or smaller sizes of olivine phenocrysts in past ejecta.

**Key words:** Volcanic ash, Shinmoe-dake, bulk ash composition, component ratio, particle size distribution.

## 1. Introduction

Ash characterization is an important method for monitoring ongoing eruptive activity and forecasting activity change (Nakada *et al.*, 1995 for Unzen volcano; Hatae *et al.*, 1997 for Kuju volcano; Taddeucci *et al.*, 2002 for Mt. Etna; Ikebe *et al.*, 2008 and Miyabuchi *et al.*, 2008 for Nakadake, Aso volcano; Rowe *et al.*, 2008 for Mount St. Helens). The main characteristic to be investigated for this purpose is the abundance and nature of juvenile material. In a situation where magmatic eruption has not begun after onset of an eruptive activity the first detection of juvenile material means that magma is rising to shallow depth. One successful example was the 1991 Unzen eruption, when juvenile material was detected in a series of ash samples before lava appeared (Nakada *et al.*, 1995). Once a large-scale magmatic eruption takes place, proximal zones at the volcano often have restricted access even if eruptive activity becomes less intensive than before. At such a time, ash could be continuously sampled in safer distal zones, allowing the tracking of eruptive activity. At the same time, juvenile material helps us judge the involvement of external water in eruptions, as magma-water interaction is recorded in surface morphology and texture of juvenile material (Miyabuchi and Ikebe, 2008; Austin-Erickson *et al.*, 2008).

Aside from examining juvenile material and related petrological and textural investigations (Taddeucci *et al.*, 2004), another benefit of monitoring ash production comes from study of the accessory material, i.e., the ash particles derived from the volcanic edifice. Such material gives insights into the crater-conduit system, including the hydrothermal system (Ohba and Kitade, 2005). Taking Showa crater of Sakurajima volcano as an example, Miyagi *et al.* (2010) showed growth and disappearance of a shallow alteration zone whose growth was promoted by fluids associated with newly intruded magma. Also, lava emplacement can be recognized as a kind of volcanic edifice modification. In the 2004–2005 eruption of Mount St. Helens, ash samples were found to include fragments of lava newly emplaced in that eruptive activity (Rowe *et al.*, 2008). Because of above developments in ash studies, it is increasingly important for all volcanologists to realize the importance and potentials of studying ash samples as described above.

We studied a series of Shinmoe-dake ash samples from the 2011 eruptive activity (January to August) and its precursory period (August 2008 to June 2010). Our focus here is not chemical characterization of juvenile material, which is separately reported in Suzuki *et al.* (2013). The data sets presented are component ratio, bulk ash composition, and particle size distribution. Bulk ash composition changes depend on proportions of ash constituents (Shimano *et al.*, 2001), while particle size distribution sometimes can be an indicator of magma-water interaction (Morrissey *et al.*,



doi:10.5047/eps.2013.02.004

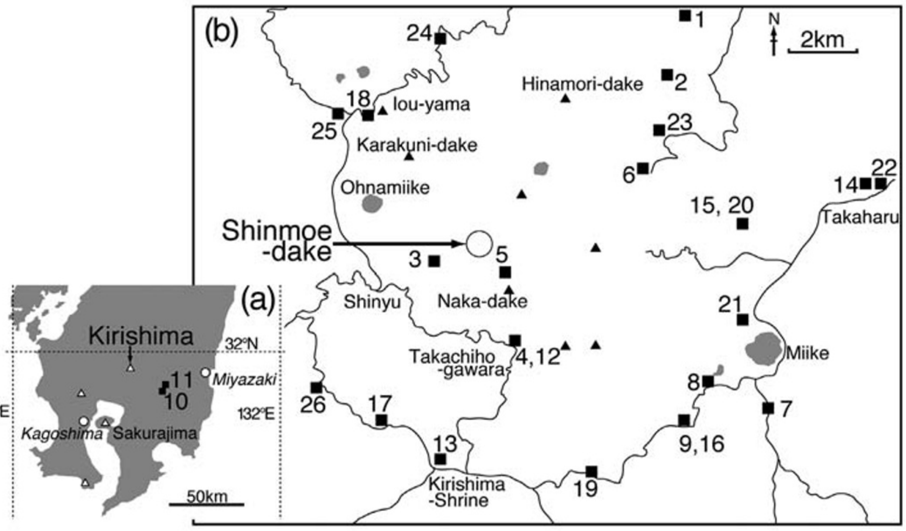


Fig. 1. Shinmoe-dake volcano in Kirishima volcano group and sampling sites. (a) Kirishima volcano group in Kyushu island, Japan, together with another Quaternary volcanoes. (b) Shinmoe-dake and another representative volcanoes in Kirishima volcano group including maars and crater lakes, along with major roads. Black squares with numbers indicate sampling sites (Site No. 1–26; also shown Table 1). Sites No. 10 and 11 are shown in (a). For isopleth maps of each event, see Nakada *et al.* (2013).

2000). The data sets, such as presence and absence of juvenile material, morphology of juvenile material and particle size distribution, partly constrain some eruptive stages proposed in Nakada *et al.* (2013). Furthermore, we show that the bulk ash composition and free-crystal ash component change at the onset of magmatic eruption in January 2011, because of the contrast between newly erupting magma and past ejecta supplying accessory material. Although data sets presented in this paper are basic and partly preliminary (e.g. particle size distribution), the summary will be useful if Shinmoe-dake becomes active again. These data sets also form a basis for future advanced studies, as described above. At the end of this paper, we again emphasize the importance of continuous observation of ash samples, taking successful Shinmoe-dake case as an example.

## 2. Shinmoe-dake 2011 Eruption and Its Background

Shinmoe-dake is one volcano in the Kirishima Volcano Group, southern Kyushu, Japan (Fig. 1). Eruptive activity of Shinmoe-dake is reported in Imura and Kobayashi (1991), but partly modified in Tsutsui *et al.* (2005). Its activity started at an unknown time before eruption of the Kobayashi pumice (16.7 cal ka BP) from Karakuni-dake (Fig. 1(b)). The present volcanic edifice of Shinmoe-dake consists of andesitic pyroclastic material interlayered with lava flows. Historical eruptions before 2008 occurred in 1716–1717, 1822, 1959 and 1991. Eruptions other than that in 1716–1717 were all phreatic. During the eruptive activity in 1716–1717 (Kyoho-eruption), multiple events repeated with pumice fall, base surge, pyroclastic flow and mud flow. The crater lava before the 2011 activity is believed to have emplaced at the end of the Kyoho-eruption.

The following descriptions of the 2011 eruptive activity are based on JMA (Japan Meteorological Agency) reports and Nakada *et al.* (2013), except where indicated. Time is in Japan standard time (JST). Here, we define phreatomagmatic eruptions as including activities caused by weakly energetic interaction of magma and external water. Precursory, small-scale phreatic eruptions occurred in August 2008 and March to June 2010. In December 2009, inflation of the volcanic edifice began to accelerate, accompanying activation of seismicity (Oikawa *et al.*, 2011; Yakiwara *et al.*, 2011). GPS data analyses by different groups, which were carried out after the January 2011 eruptions, commonly attributed the inflation to a spherical source 7.5 km deep (GIAJ, 2012) or 9.2 km deep (Nakao *et al.*, 2013) and 7–8 km NW of Shinmoe-dake.

The next phase of activity started on 19 January 2011 with a phreatomagmatic eruption. Then, a series of magmatic eruptions started on January 26, 2011. Activity in this period was most intensive and most voluminous. Three sub-Plinian events occurred, starting at 14:49 on the 26th, about 2:00 on the 27th, and 15:41 on the 27th. Each event lasted a couple of hours (Ichihara *et al.*, 2012, http://outreach.eri.u-tokyo.ac.jp/eqvolc/201101_shinmoe/eng/#MTSAT). The total tephra mass for the three events is 16–30 $\times$ $10^6$ ton (DRE, 6.4–12$\times 10^6$ $m^3$) (Maeno *et al.*, 2012). Doppler radar analyses showed echo heights of plumes reached 8.5 km a.s.l. in all of the three events (Shimbori and Fukui, 2012). The borehole tilt measurements recorded three syneruptive step-wise deflations corresponding to each sub-Plinian event (Ueda *et al.*, 2013; source depth of 9.8 km located 7–8 km NW of Shinmoe-dake). New lava dome was discovered in the crater in the morning of 28 January, but later satellite-image analyses (e.g. Ando, 2012; Ozawa and Kozono, 2013) determined that lava emplacement had already started at 22:53 on the 27th. The lava dome grew rapidly to have a diameter of 500 m by the evening of the 29th, filling the original crater (we thus call it accumulated lava). The lava volume stayed almost unchanged thereafter, reaching a final value of 14–18 $\times$ $10^6$ $m^3$ (Sasaki *et al.*, 2011; GIAJ, 2012; Kozono *et al.*, 2013). The lava emplacement was accompanied by explosions, one of which occurred at

Table 1. Sampling conditions and purpose of use for ash samples.

| Eruption year, date and time, and plume height [a] | | | | Sampling | | | | Preparation | Purpose [f] | | |
|---|---|---|---|---|---|---|---|---|---|---|---|
| Year | Date and time | Corresponding event | Plume height(m) | Collected by [c] | Date and time | Site ( Fig.1) | Condition [e] | Filtration [e] | Component [g] | Bulk | Size |
| 2011 | Aug 31, 2:43~Sep 6, 13:50 | — | 500 | ERI, NIED, T. Kobayashi | Sep 1, 14:00 | 26 | Dry | No | OK | OK | OK |
| 2011 | Aug 6, around 9:41 and 18:29 | — | No data | Kirishima Geopark | Aug 7 | 25 | Wet(slight) | No | OK(125-250μm) | OK | OK |
| 2011 | Jun 29, 10:27~Jul 1, 1:21 | — | 1000 | JMA | Jun 29, 11:40 | 24 | Dry | No | OK | OK | OK |
| 2011 | Jun 23, 20:49 | — | 200 | JMA | Jun 24, 11:20 | 23 | Dry | No | OK(125-250μm) | — | OK |
| 2011 | Jun 16, around 18:05 | — | No data | Takaharu-cho | Jun 17, 12:00 | 22 | Dry | No | OK(ca.100μm) | — | — |
| 2011 | Apr 18, 19:22 | — | 2000 | ERI | Apr 19, 14:00 | 21 | Dry | No | OK(500-1000μm) | OK | OK |
| 2011 | Apr 3, 8:41 | — | 3000 | ERI | Apr 4, 16:00 | 20 | Dry | No | OK | OK | OK |
| 2011 | Mar 13, 17:45 | — | 4000 | ERI | Mar 13, 18:40 | 19 | Dry | No | OK | OK | OK |
| 2011 | Feb 24, 3:38 | — | Unknown | ERI and NIED | Feb 24, 11:30 | 18 | Snow | Yes | OK | OK | OK |
| 2011 | Feb 18, 18:16 | — | 3000 | JMA | Feb 18, 20:25 | 17 | Dry | No | OK | OK | OK |
| 2011 | Feb 7, 14:20~Feb 8, 12:30 | — | Unknown | H. Sato | Feb 7, 14:20~Feb 8, 12:30 [d] | 16 | Dry | No | OK | — | OK |
| 2011 | Feb 2, 10:47 § | 7th vulcanian explosion | >500 | M. Sakagami | Feb 2, 11:10~11:20 [d] | 15 | Dry | No | OK | — | OK |
| 2011 | Jan 28, 17:20 | Deposited on Jan28 [b] | >1000 (12:47) | ERI, NIED | Jan 28, 17:20 | 14 | Dry | No | OK | OK | OK |
| 2011 | Jan 27, 15:41 § | The 3rd sub-Plinian [b] | 3000(17:35) | ERI, NIED | Jan 28, 13:45 | 13 | Dry | No | OK | OK | OK |
| 2011 | Jan 27, 12:15~12:43 | Repose of sub-Plinian event | 1000 (afternoon) | NIED | Jan 27, 12:15~12:43 [d] | 12 | Dry | No | OK | OK | OK |
| 2011 | Jan 26, 15:30~ § | The 1st sub-Plinian | 2000 (18:50) | J. Hirabayashi | Jan 26, 19:30 [d] | 11 | Dry | No | — | OK | — |
| 2011 | Jan 26, 15:30~ § | The 1st sub-Plinian | 2000 (18:50) | J. Hirabayashi | Jan 26, 18:30~19:00 [d] | 10 | Dry | No | OK(500-1000μm) | OK | — |
| 2011 | Jan 26, around 14:30 | Precursory of 1st sub-Plinian | Unknown | M. Ukawa | Jan 26, 14:30 [d] | 9 | Dry | No | OK(125-500μm) | — | — |
| 2011 | Jan 19, 1:27 | — | No data | JMA | Jan 19, 12:30 | 8 | Dry | No | OK | OK | — |
| 2011 | Jan 19, 1:27 | — | No data | T. Kobayashi | Jan 20 | 7 | Dry | No | — | OK | OK |
| 2010 | Jun 27, around 1:35/Jun 28, 16:02 | — | No data | R. Imura | Jun 29 | 6 | Wet, leaves | Yes | OK [h] | — | — |
| 2010 | May 27, 15:36 | — | >100 | T. Kobayashi and Y. Tajima | May 30 | 5 | Grasses | Yes | OK | — | OK |
| 2010 | May 27, 15:36 | — | >100 | JMA | May 27 | 4 | Dry | No | OK [h] | — | — |
| 2010 | Mar 30, around 8:00 | — | 400 | K. Aizawa | Mar 31 | 3 | Dry | No | OK | OK | OK |
| 2008 | Aug 22, 16:34 | — | No data | T. Kobayashi | Aug 24 | 2 | Wet, leaves | Yes | OK(350-500μm) | OK | OK |
| 2008 | Aug 22, 16:34 | — | No data | JMA | Aug 23, 15:58 | 1 | Wet | Yes | OK(350-500μm) | OK | — |

[a] Based on JMA reports. For January 26 to February 9, when eruption was continuous for the longest time, either start time of corresponding event (if associated with significant intensity change, as noted with §) or sampling time is shown. For this period, the corresponding event name is shown on the right, if necessary. For other periods, only the start time of the event is known in most cases. "No data" indicates plume height could not be obtained because of bad weather. Time is shown if the plume height data is from specific time.

[b] Judged based on distribution of ejecta (also see Nakada *et al*., 2013 , this-issue).

[c] ERI, Earthquake Research Institute; JMA, Japan Meteorological Agency, NIED, National Research Institute for Earth Science and Disaster Prevention.

[d] Sampled during each event.

[e] Noted for samples which needed recovery of all ash particles from plastic sample bag and filtration to remove deionized water (for detail, see 4.1). Labels leaves, grasses and snow indicate the medium on which ash was deposited; Wet, ash was wet probably due to rain.

[f] "OK" indicates sample was used for the purpose shown in the column header, including component analyses, bulk ash composition (XRF) and particle size distribution.

[g] 250-500μm size fraction was used except for some samples with size information.

[h] Measured particle number was small due to limited amount of sample. So, data were used only for description (5.1.2) and are not shown in Fig. 2.

12:47 on 28 January. Along with the borehole tilt measurement, the GPS network recorded rapid deflation during the sub-Plinian events and the lava accumulation. The deflation could be explained by almost the same sources as the pre-eruptive period but at a slightly shallower depth; 6.2 km (GIAJ, 2012) and 8.4 km (Nakao *et al*., 2013). The total volume of deflation is $11.7–15.2 \times 10^6$ m$^3$ (Nakao *et al*., 2013) or $10–11.8 \times 10^6$ m$^3$ (GIAJ, 2012). Inflation resurged soon after the end of January 2011.

The lava emplacement was followed by vulcanian explosions that ejected blocks of "the lava accumulated in January" from the crater, along with ash. An explosion at 7:54 on 1 February brought a lava block of 70 cm long (calculated to be 1–3 ton; Maeno *et al*., 2013) to a location of 3.2 km SW from the crater. The eruption after 9 February became less frequent and discontinuous (5 times for the rest of February, 7 times in March, 3 times in April). After two months repose, five phreatomagmatic eruptions were recorded between the middle of June and early September. Inclusion of longer time events between June and September compared with the previous stage (Table 1) is a reason not to recognize this period as vulcanian stage. At the time of writing, no eruption has been noted since September 2011. According to GPS data, inflation continued until December 2011 at a similar rate to that during the pre-eruption period (December 2009 to January 2011). Magma accumulation in the reservoir seems to have recovered to a similar level as was reached in January 2011.

## 3. Samples

The samples and sampling conditions are summarized in Table 1, and sampling sites are shown in Fig. 1. The examined eruptions cover the entire 2011 eruptive activity (January to August 2011) and its precursory stage (August 2008 to June 2010). Plume heights in corresponding events are also summarized in Table 1. We indicate each sample by eruption date, together with eruption time and site number, if necessary. Most samples were collected at the time of deposition or by the next day. Sampling sites are within 10 km of Shinmoe-dake crater (Fig. 1(b)), except for two sites about 25 km from the crater (Fig. 1(a)). For eruptions with multiple samples for ash distribution and total volume of ejecta (Nakada *et al*., 2013), samples from the sites closest to the crater and the dispersal axis were used. Ash samples were collected by the following means: a) placing plates or paper on a flat surface for some period (e.g. 18:30–19:00 January 26, February 2, February 7–8, all 2011 eruptions); b) from surface of artificial material including monitoring device and edge of low-traffic road; and c) together with snow, leaves and grass on which ash particles were deposited (Table 1, condition). The original weights of samples in this study varied approximately between 1 g and 100 g, depending on scales of the eruptions.

## 4. Methods

### 4.1 Collecting all ash particles from a plastic sample bag

Wet samples and samples collected with plants and snow (see Table 1) required this preparation step. At first, all ash particles in the bag were emptied into beakers using deionized water. Ash particles adhering to leaves and grass were removed using a new toothbrush. Next, deionized water with ash particles was filtered to remove water, and the filter paper and remaining ash particles were completely dried in an oven at 110°C. Ash particles were separated from the filter paper using a new toothbrush. Finally, the ash particles were homogenized by mixing well, and remaining fragments of plants were removed with a pincette under a binocular microscope.

### 4.2 Analytical methods

Component analyses were conducted for almost all samples, and a reduced number was examined for bulk ash composition and particle size distribution (Table 1), usually due to limitation in sample amount. Bulk ash compositions were determined by X-ray fluorescence (XRF) (RIGAKU ZSX Primus II) at Earthquake Research Institute (ERI), University of Tokyo, using glass beads with five parts flux to one part sample.

The characterization of both ash component and particle-size distribution commonly required two preparation processes, 1) ultrasonic cleaning, and 2) sieving. Typically a few grams were extracted from the original sample and weighed. The precision of weighting was 0.001 g. Then the sample was poured into deionized water in a beaker. Submerging the beaker in an ultrasonic bath, the upper portion of water including only fine ash particles (<several tens of $\mu$m) was removed. The ultrasonic cleaning and removal were repeated until the upper portion was transparent even during ultrasonic cleaning. The coarse part of the sample remaining in the beaker was dried completely at 110°C and was weighed to yield the weight, by difference, of the removed fine part (<several tens $\mu$m). The weight of the fine part was later used to yield a particle size distribution (in wt%). The removal of the fine part also aids the observation of coarser particles under the binocular microscope for component analyses.

For particle size analyses, the coarse part (>several tens of $\mu$m) collected during the previous procedure was separated into five size fractions by hand sieving; several tens–125 $\mu$m, 125–250 $\mu$m, 250–500 $\mu$m, 500–1000 $\mu$m and >1000 $\mu$m fractions. Each size fraction was weighed to obtain the final particle size distribution in wt%.

Ash component analyses were carried out for 24 samples (Table 1). Depending on the amount of the original sample and the resultant number of classified particles, the use of the ash component data differs. We yielded the ash-component percentage (in number, thus data shown in vol%) of 22 samples for which classified particles numbered several hundred or more (Table 2; Fig. 2), while we just calculated a rough ash-component ratio for the two others (May 27 and June 27–28, 2010; Table 1) to compare the May 27 and June 27–28 samples with other samples of similar eruption dates. Size fractions of 250 to 500 $\mu$m were the target of component analyses in most samples (Table 1), because the particles of that size range are easy to classify with pincette and additionally the size range has relatively abundant particles. In each sample, no clear difference of ash component was found among different size fractions.

## 5. Analytical Results

### 5.1 Results of component analysis

**5.1.1 Classification of ash particles and overall results** All ash samples contain one or more of the following components: 1) pumice, 2) scoria, 3) lava, 4) altered material, 5) free-crystal (Fig. 2 and Table 2). Not only pumice and scoria particles, but also some of the lava particles are glassy regardless of the eruption stage (e.g. Figs. 3, 5(b), 6, 7(a)–(c), 8). Accordingly, pumice+scoria particles and lava particles were distinguished by vesicularity. Lava particles typically have fracture planes forming the surface, different from most scoria and pumice particles (one exception is January 19, 2011 pumice explained below). We use color as the difference between pumice and scoria: white, light gray and light brown for pumice (Figs. 3, 5(a), 6, and 10); black and dark brown for scoria (Figs. 3, 4, 6, 9). Generally, pumice particles have higher vesicularities than scoria particles. We further define ash components other than "free-crystal" as follows.

1) "Altered material" comprises the particles with the highest degree of alteration of all ash components. Surfaces of typical "altered material" are mostly or completely altered and have an orange or white color (e.g. Fig. 3). The white ones probably resulted from silicification and are often accompanied by small sulfides (Fig. 3). When the origin of "altered material" can be identified and it is either pumice or scoria; vesicles are completely filled with the orange or white alteration product.

2) "Pumice" and "scoria" particles were further classified into "fresh" and "partly altered" sub-types (Fig. 2 and Table 2), according to the degree of freshness. We regard only "fresh" ones as "juvenile material". The degree of freshness is judged high, 1) if vitreous luster is recognized on the particle surface, and 2) if abrasion on the particle surface is free or slight, and 3) if the particle surface and vesicles are free from adhering alteration product. Most "pumice" and "scoria" particles in the 2011 ash samples are the "fresh" sub-type (Fig. 2, Table 2).

3) Lava particles were further classified into "fresh" and "partly altered" sub-types (Fig. 2 and Table 2). The degree of freshness is judged using the same criteria as for scoria and pumice. Particle shape is angular in the "fresh" sub-type but subangular in the "partly altered" sub-type (e.g. Fig. 7), because of an increasing degree of surface abrasion. We regard "partly altered" lava particles as accessary or accidental. But, the origin of "fresh lava" requires some discussion (Subsection 6.2). Examples of "partly altered" particles are in Figs. 3 and 7(d), while those of "fresh" particles are in Figs. 5(b), 6, 7(a)–(c), and 8. Only "partly altered" lava particles are recognized in ash samples issued between 2008 and 2010, and "fresh" lava particles first appear on

Table 2. Component analysis data for ash samples.

| Eruption[a] | | Component percentage (normalized to 100 vol%) | | | | | | | | | Total |
|---|---|---|---|---|---|---|---|---|---|---|---|
| Day and time | Year | 1) Pumice | | 2 ) Scoria | | 3) Lava | | | 4) Altered | 5) Free | particle N |
| | | fresh[b] | partly altered | fresh[b] | partly altered | fresh[c] | partly altered | unclassified[d] | material | crystal | counted |
| Aug 31 | 2011 | 0.0 | 0.0 | 4.5 | 0.0 | – | – | 79.4 | 3.4 | 12.7 | 683 |
| Aug 6 | 2011 | 0.4 | 0.0 | 0.3 | 0.0 | – | – | 62.0 | 14.3 | 23.0 | 686 |
| Jun 29 | 2011 | 6.9 | 2.2 | 7.4 | 4.0 | – | – | 43.2 | 24.7 | 11.6 | 405 |
| Jun 23 | 2011 | 1.7 | 0.0 | 2.4 | 0.0 | – | – | 47.1 | 22.7 | 26.1 | 533 |
| Jun 16 | 2011 | 0.7 | 0.0 | 0.3 | 0.0 | – | – | 68.8 | 3.3 | 26.9 | 301 |
| Apr 18 | 2011 | 0.0 | 0.0 | 1.7 | 0.0 | 71.0 | 16.1 | – | 5.4 | 5.8 | 708 |
| Apr 3 | 2011 | 3.1 | 0.0 | 2.5 | 0.0 | 49.9 | 22.8 | – | 3.3 | 18.4 | 675 |
| Mar 13 | 2011 | 1.7 | 0.0 | 8.0 | 0.0 | 42.8 | 22.7 | – | 11.1 | 13.6 | 287 |
| Feb 24 | 2011 | 0.4 | 0.0 | 15.0 | 0.0 | 52.9 | 15.6 | – | 4.6 | 11.6 | 889 |
| Feb 18 | 2011 | 0.3 | 0.0 | 6.0 | 0.0 | 58.2 | 15.1 | – | 5.0 | 15.5 | 1119 |
| Feb 7~8 | 2011 | 0.6 | 0.0 | 3.1 | 0.0 | 59.0 | 21.9 | – | 1.9 | 13.6 | 360 |
| Feb 2 | 2011 | 0.3 | 0.0 | 0.0 | 0.2 | 42.7 | 30.8 | – | 2.3 | 23.8 | 572 |
| Jan28, ~17:20 | 2011 | 9.3 | 0.0 | 11.6 | 0.0 | 27.3 | 17.5 | – | 14.0 | 20.3 | 713 |
| Jan27, 15:41~ | 2011 | 37.4 | 0.6 | 10.9 | 0.6 | 18.2 | 9.3 | – | 5.7 | 17.4 | 688 |
| Jan27, noon | 2011 | 0.2 | 0.0 | 0.5 | 0.1 | 18.5 | 51.8 | – | 6.3 | 22.7 | 1079 |
| Jan26, ca.19:00 | 2011 | 37.5 | 0.0 | 6.3 | 0.3 | 17.1 | 12.8 | – | 11.2 | 14.8 | 1595 |
| Jan26, 14:30 | 2011 | 0.0 | 0.5 | 0.1 | 0.2 | 0.0 | 24.7 | – | 49.4 | 25.1 | 822 |
| Jan 19 | 2011 | 7.7 | 0.5 | 0.6 | 3.3 | 4.3 | 44.6 | – | 21.5 | 17.5 | 636 |
| May 27 | 2010 | 0.0 | 1.2 | 0.6 | 1.4 | 0.0 | 27.2 | – | 52.4 | 17.1 | 496 |
| Mar 30 | 2010 | 0.0 | 0.4 | 0.4 | 2.7 | 0.0 | 47.9 | – | 31.1 | 17.4 | 447 |
| Aug 22 (Site 2) | 2008 | 0.1 | 1.4 | 0.0 | 2.8 | 0.0 | 25.3 | – | 65.2 | 5.3 | 1840 |
| Aug 22 (Site 1) | 2008 | 0.0 | 3.2 | 0.0 | 9.5 | 0.0 | 23.3 | – | 59.5 | 4.7 | 602 |

Target sizes of analyses are shown in Table1 and Fig. 2. For definition of each component, see 5.1.1.

[a] Corresponding to notation in Fig. 2. For more detail of each eruption, see Table1 and Section 2.

[b] Juvenile material.

[c] Corresponding to either dense part of the juvenile material or lava accumulated in the crater (after the night of January 27, 2011; see section 6.2).

[d] Due to possible alteration of lava accumulated in the crater (see "second phreatomagmatic stage" in 5.1.2).

January 19, 2011 (Fig. 2 and Table 2). As seen in the figures, the "fresh" and "partly altered" lava particles have different color variations, and the "fresh" sub-type has a higher ratio of glassy particles. Binocular microscope observation revealed different phenocryst assemblages for the two lava sub-types; olivine + two pyroxenes + plagioclase + Fe-Ti oxides in "fresh lava", and two pyroxene+plagioclase+Fe-Ti oxides in "partly altered lava". This was also confirmed by thin section observations.

The assemblages of the free-crystal component shift from two pyroxenes + plagioclase + Fe-Ti oxides before June 2010 to olivine+two pyroxenes+plagioclase+Fe-Ti oxides in the 2011 eruptions.

### 5.1.2 Ash component characteristics in each eruptive stage

*August 2008 to June 2010 (phreatic stage).*

Figure 3 shows the typical variety of ash components. "Altered material" is the dominant component (65–30 vol%), "partly altered lava" is next (25–50 vol%), and "partly altered pumice + scoria"occurs in small amounts (Table 2 and Fig. 2). The percentage of "altered material" in this stage is the highest through the whole activity. Furthermore, most particles in the "altered material" class have a completely altered surface. Most of "pumice" and "scoria" particles are "partly altered" sub-types, i.e. non-juvenile (e.g. pale yellow pumice, in Fig. 3-1). "Fresh scoria" particles (possibly juvenile), with a vitreous surface luster (Figs. 3-2 and 4) are found in ash samples of March 2010 and afterward, but they account for only <1 vol% of whole ash (Table 2 and Fig. 2). All lava particles are the "partly-altered" sub-type.

*January 19, 2011 (phreatomagmatic stage).*

The clear differences from the previous stage are the appearances of considerable amounts of "fresh pumice (juvenile)" (7.7 vol%) and glassy "fresh lava" (4.3 vol%) (Table 2 and Fig. 2). Free-crystals of olivine appeared for the first time since August 2008. Other components are unchanged: 1) a slight amount of "fresh scoria" (<1 vol%) can be judged juvenile, 2) the presence of "partly altered" lava particles of similar appearance to those of the previous stage (Fig. 3(a)). The "fresh pumice" particles (Figs. 5(a) and (c)) are free from alteration and adhering fine alteration products in vesicles. The "fresh pumice" particles are white (Fig. 5(a)) and have relatively-low vesicularity and blocky shape (Fig. 5(c)).

*January 26–28, 2011 (sub-Plinian events and following explosion).*

The five analyzed samples may be classified into two groups; January 26, 14:30 (just prior to the first sub-Plinian event) ash and the remainder (Fig. 2; Table 2). The first ash sample resembles those of August 2008–June 2010 rather than that of January 19, 2011. "Altered material" again dominates, and most of the "pumice", "scoria", and "lava" particles are partly altered and non-juvenile.

The other January 26–28 samples also differ from that of January 19. Most "scoria" and "pumice" are fresh (i.e. juvenile). The amounts of "fresh pumice", "fresh scoria" and "fresh lava" are greater than on January 19, and the amounts of "partly altered lava" and "altered material" smaller (Fig. 2 and Table 2). The total of juvenile pumice and scoria is the highest in the two sub-Plinian events (∼50 vol%) of January 26 and 27. The amount of

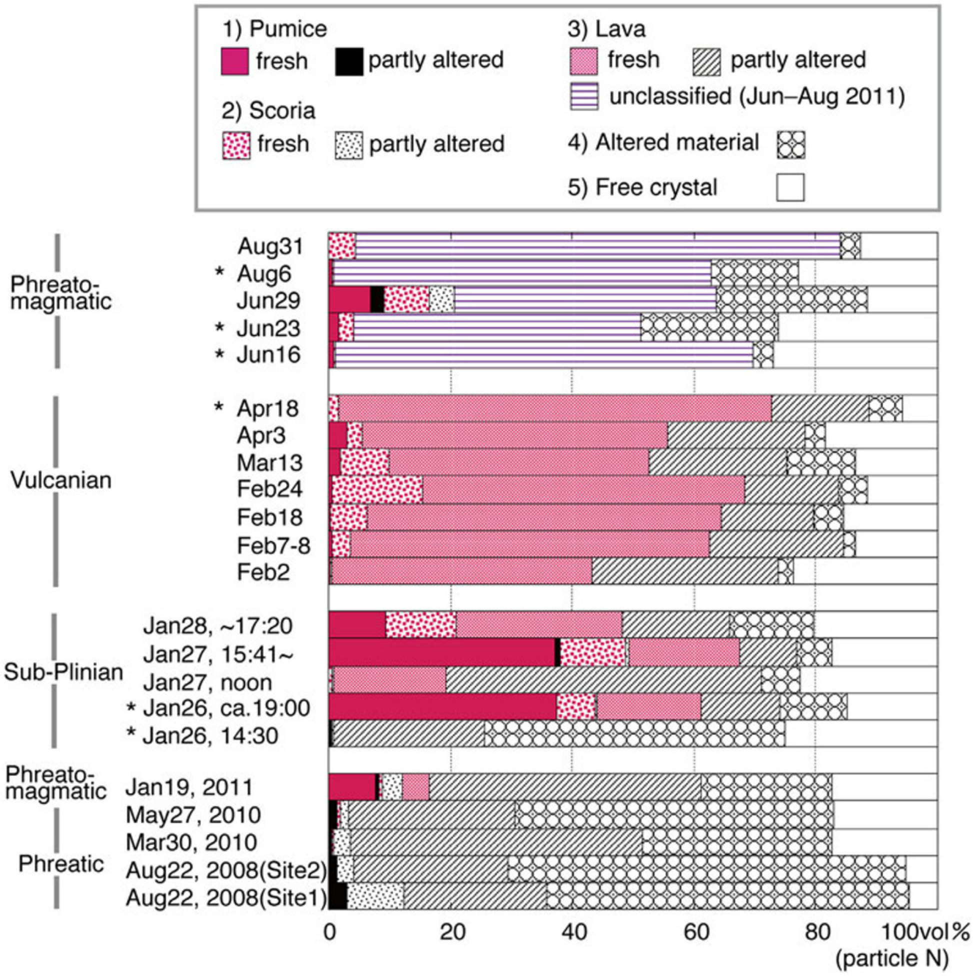


Fig. 2. Temporal change of ash components during 2011 eruption (January 19–August 31) and its precursory stage (August 2008–May 2010). For definition of each component, see Subsection 5.1.1. Original percentage data and total number of particles counted are listed in Table 2. Target size was either 250–500 $\mu$m or 350–500 $\mu$m (two samples of August 22, 2008), except for 6 samples with star (*); January 26, 14:30, 125–500 $\mu$m; January 26, ca. 19:00, 500–1000 $\mu$m; April 18, 500–1000 $\mu$m; June 16, ca. 100 $\mu$m; June 23, 125–250 $\mu$m; August 6, 125–250 $\mu$m (Table 1). Two samples of August 22, 2008 can be distinguished by Site No. (also shown in Fig. 1 and Table 1). Rose-colored bars represent particles that came directly from 2011 magma (6.2; Table 2). Unlike the vulcanian stage, lava particles from the second phreatomagmatic stage (June 16 to August 31, 2011) were not classified further, because of possible alteration of lava accumulated in the crater (second phreatomagmatic stage in 5.1.2). **Color version available online**.

"fresh lava" is almost constant (about 20–30 vol%). The "fresh lava" particles are mostly glassy with a vitreous surface luster and are olive, pale-brown, gray, black and pale-green. The color variation resembles that of the "scoria" and "pumice"(Fig. 6). The vesicularities of the "fresh lava" particles range continuously to those of "fresh scoria" and "fresh pumice".

*February to mid-April, 2011 (vulcanian stage).*

Noteworthy characteristics of this period are the high percentage of the "lava" component (65–85 vol%) and the high ratio (60–80 vol%) of fresh lava (Fig. 2 and Table 2). The amount of "altered material" is generally smaller than in previous periods. The maximum total of "fresh pumice" and "fresh scoria" in this stage (15.4 vol% on February 24) is smaller than on January 28 (20.9 vol%) and January 26–27 (43.8 and 48.3 vol%).

"Fresh lava" particles have similar color variations to those in the sub-Plinian stage (e.g. Figs. 6 and 7(a)–(b)). But, oxidized lava particles appear for the first time in this stage (Fig. 7(c)) and are observed on most eruption dates. The oxidized ones are categorized into "fresh lava" particles because unoxidized parts in each grain have similar appearance as fresh lava particles; the oxidation occurred synerup-tively. In most samples, the occurrence of oxidized "fresh lava" correlates with that of oxidized "fresh scoria" (e.g. Fig. 9(a)), which also appears for the first time in this stage. "Fresh lava" particles in ash erupted on and after February 24 have patches of slight alteration (e.g. Fig. 8). The "fresh pumice" particles account for <3 vol%, highest on March 13 and April 3. The amount of "fresh scoria" increases until February 24 and then decreases, in the range of <15 vol%. In eruptions for which plume heights are available (Table 1), the "fresh scoria" abundance (Table 2) decreases with decrease in height; 8 vol% and 4000 m (March 13), 6 vol% and 3000 m (February 18), 2.5 vol% and 3000 m (April 3) and 1.7 vol% and 2000 m (April 18). The "fresh scoria" particles erupted on April 18 might have been recycled from juvenile scoria particles erupted previously, as follows. They are tentatively classified as "fresh scoria" because of the vitreous luster of vesicle walls, but their surfaces are abraded

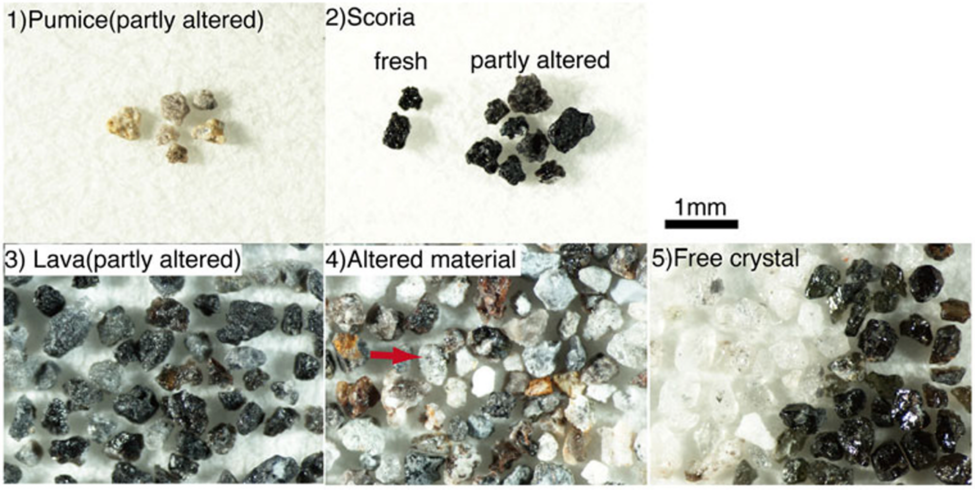


Fig. 3. 250–500 $\mu$m fraction of May 27, 2010 ash (collected at Site No. 5; Fig. 1 and Table 1). For definition of each ash component, see Subsection 5.1.1. All photographs were taken under binocular microscope at the same magnification. "Partly altered pumice" particles having pale-yellow color are not juvenile. In "scoria", only "fresh" ones can be recognized as juvenile. A higher magnification photograph of the "fresh scoria" is shown in Fig. 4. "Partly altered lava" particles (accessory) are less altered and more angular in comparison with "altered material". In "altered material", white-colored particles were probably generated by silicification and are charged with small sulfides (red arrow). Orthopyroxene, clinopyroxene and plagioclase are recognized as the "free-crystal" component. **Color version available online**.

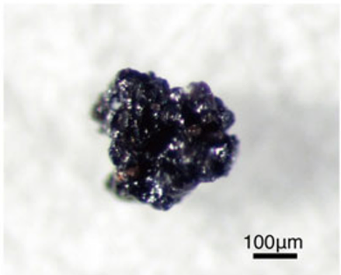


Fig. 4. A juvenile "fresh scoria" particle from 250–500 $\mu$m fraction of May 27, 2010 ash (collected in Site No. 5; Fig. 1 and Table 1). Photograph taken under binocular microscope. For criteria to discriminate between juvenile and non-juvenile, see Subsection 5.1.1. **Color version available online**.

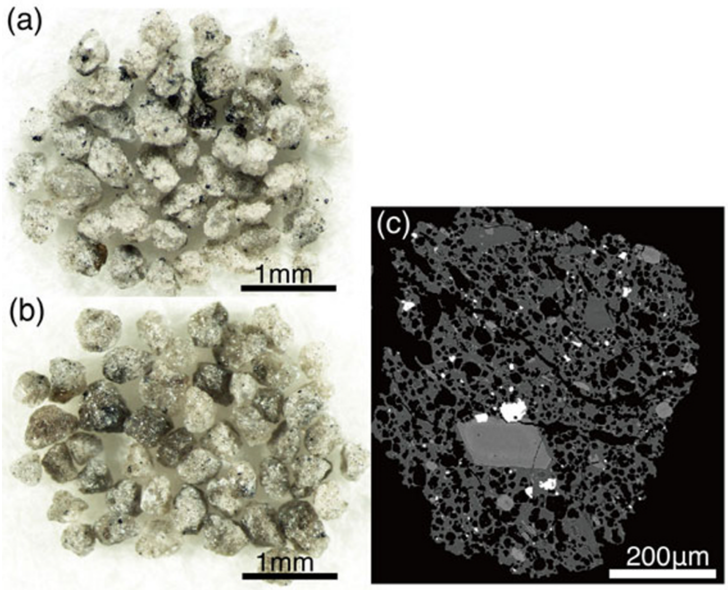


Fig. 5. Juvenile "fresh pumice" ((a) and (c)) and "fresh lava" (b) in January 19, 2011 ash (collected at Site No. 8; Fig. 1 and Table 1). (a) and (b) are from 250–500 $\mu$m fraction, while (c) is from 500–1000 $\mu$m fraction. (a) and (b) are photographs taken under binocular microscope, while (c) is BSE image of thin section. For definition of each ash component, see Subsection 5.1.1. Note denser "fresh lava" particles have darker color than fresh pumice particles ((a) and (b)). As shown in (c), the "fresh pumice" has low vesicularity and blocky shape, implying magma interaction with aquifer. In (c), pyroxene and Fe-Ti oxide phenocrysts are present. Like the "fresh pumice" particles, "fresh lava" particles in (b) are glassy. **Color version available online**.


Fig. 6. Fresh scoria, pumice and lava particles (500–1000 $\mu$m fraction) in ash from the first sub-Plinian event (deposited at Site No. 10 between 18:30 and 19:00 on January 26, 2011; Fig. 1 and Table 1). All are photographs taken under binocular microscope at the same magnification. For definition of each ash component, see Subsection 5.1.1. Both the "fresh pumice" and "fresh scoria" are juvenile. The "fresh lava" particles are glassy and have similar color variation as "fresh pumice" and "fresh scoria". The "fresh lava" particles have similar petrographical characteristics as pumice and scoria, so these are judged as a part of the erupting magma (Subsection 6.2). **Color version available online**.

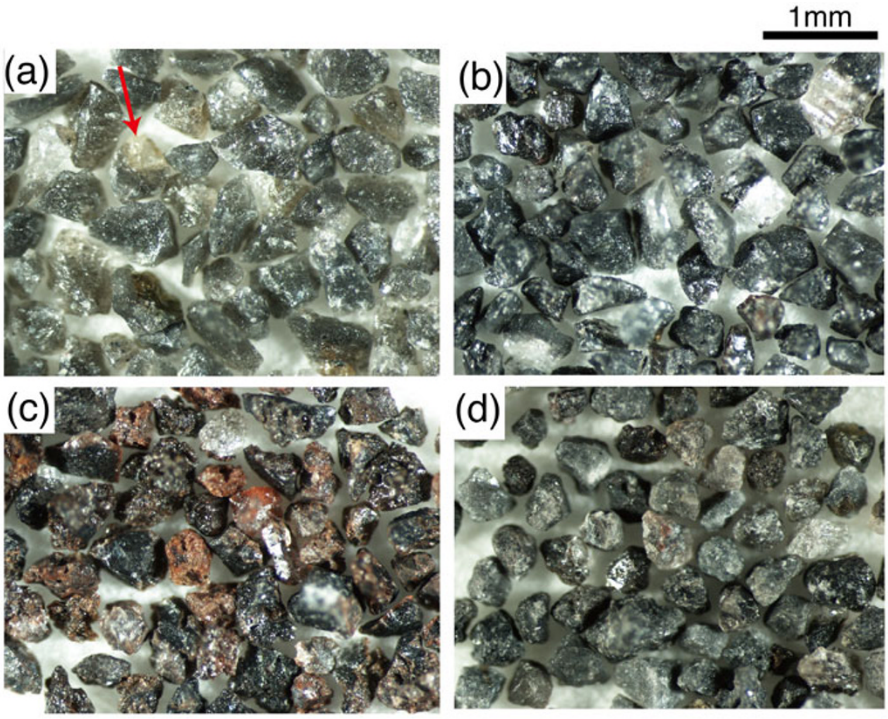


Fig. 7. Typical variation of "lava" particles in early phase of vulcanian stage (February to mid-April). 250–500 $\mu$m fraction of February 18, 2011 ash (Table 1). All are photographs taken under binocular microscope at the same magnification. For definition of "lava" particles and its sub-types ("fresh" and "partly-altered"), see Subsection 5.1.1. (a)–(c) are "fresh lava" (corresponding to either lava accumulated in the crater during the 2011 eruptive activity (Section 2) or vesicle-poor part of erupted magma), while (d) is "partly altered lava". Note the different appearance between "fresh lava" and "partly altered lava"; "fresh lava" particles are more angular and have luster on particle surface. Oxidized particles are identified in (c). "Fresh lava" particles commonly include olivine phenocrysts (Subsection 5.1.1), and one example is seen in (a) (red arrow). **Color version available online**.


Fig. 8. Lava particles in April 3, 2011 ash (250–500 $\mu$m fraction) which were classified into "fresh lava" because of similar appearance to "fresh lava" particles in February to March vulcanian ash samples (e.g. Figs. 7(a)–(b)). However, "fresh lava" particles in April 3 ash are partly altered (red arrows). The photograph was taken under binocular microscope. For definition of lava particles and its sub-types ("fresh" and "partly-altered"), see Subsection 5.1.1. **Color version available online**.

(Fig. 9(b)). In any case, two months dormancy started when the juvenile content became low (1.7 vol% on April 18; Table 2 and Fig. 2).

*Mid-June to August 2011 (second phreatomagmatic stage).*

Lava particles erupted during this time are not classified into sub-types, because the following observations make us consider sub-types as no longer meaningful. "Fresh lava" particles in the late vulcanian stage have slight alteration (Fig. 8), and the mid-June eruption occurred after a two-month repose (Section 2) during which progressive alteration of crater lava is plausible. Otherwise, ash component ratios in this stage are similar to those in the vulcanian stage (Fig. 2, Table 2). The total of "fresh pumice" and "fresh scoria" particles shows a pattern characterized by increase and later decrease, peaking at ca. 15 vol% on June 29. The "fresh pumice" and "fresh scoria" particles early in this period have fluidal shapes as if a splash of magma was quenched instantly at ejection (Fig. 10, example of June 23). The shapes are quite different from those of the April 18 "fresh scoria", with significant surface abrasion (previous section; Fig. 9(b)). This strongly suggests that the June 23 "fresh pumice" and "fresh scoria" are juvenile. The amount of "altered material" in this stage is slightly higher than in the vulcanian stage (especially until August 6), regardless of the observed ash size fraction (Fig. 2).

## 5.2 Bulk ash composition

Figure 11 shows bulk ash $SiO_2$ contents as a function of eruption date. Ash samples from the August 22, 2010 eruption have maximum $SiO_2$ contents (64.4–66.3 wt%). There is a gap in the data between the August 22 ash samples and the remainder. Samples of March 30, 2010 and January 19, 2011 have the highest $SiO_2$ contents after August 22, 2008 (60.3–60.5 wt%).

In the $SiO_2$ variation diagrams (Fig. 12), the bulk ash

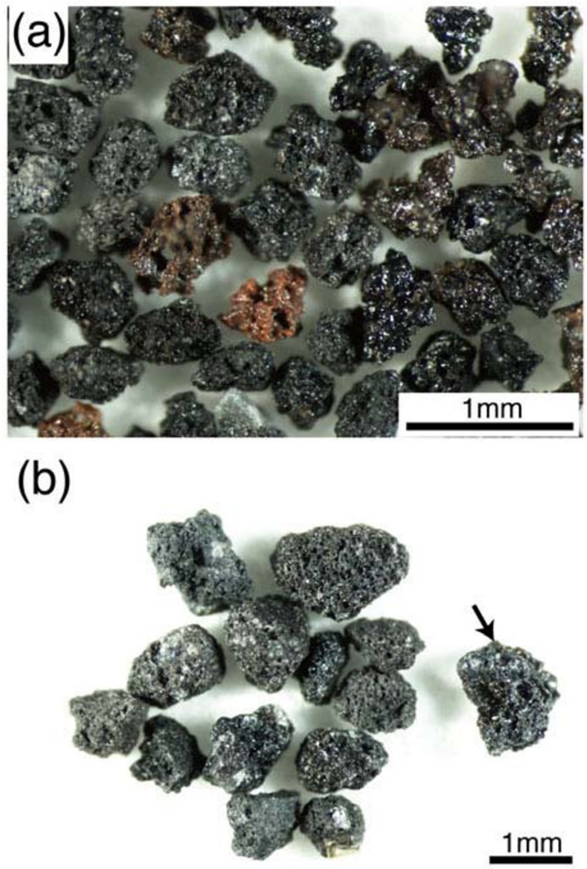


Fig. 9. Examples of juvenile "fresh scoria" particles in vulcanian ash. Both photographs were taken under binocular microscope. For definition of "scoria" particles and its sub-types ("fresh" and "partly-altered"), see Subsection 5.1.1. (a) shows "fresh scoria (juvenile)" particles in February 18 ash (250–500 $\mu$m fraction). Some of the "fresh scoria" particles are oxidized, similar to coexisting "fresh lava" particles (Fig. 7(c)). Degree of surface luster of unoxidized particles is variable. (b) shows "scoria" particles in April 18 ash (500–1000 $\mu$m fraction). These were classified into "fresh scoria" (Table 2; Fig. 2) because of luster inside vesicles (e.g. particles with arrow) and resemblance to "fresh scoria particles" in previous eruptions (e.g. Fig. 9(a)), although surfaces of particles in (b) are abraded. **Color version available online**.

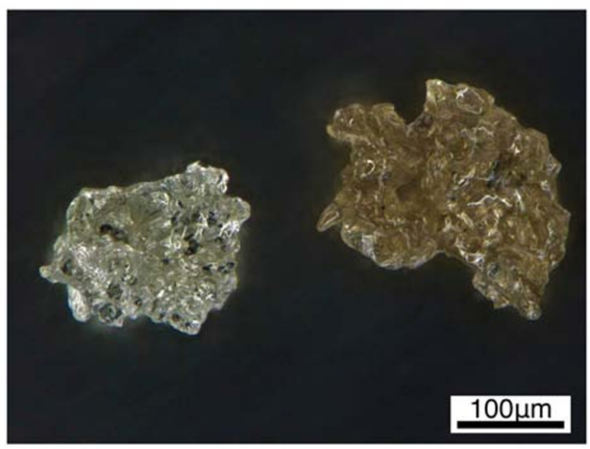


Fig. 10. "Fresh pumice (juvenile)" particles in 125–250 $\mu$m fraction of June 23, 2011 ash. The photograph was taken with digital microscope. For definition of "pumice" particles and its sub-types ("fresh" and "partly-altered"), see Subsection 5.1.1. The particles look white (left) or light brown (right) under binocular microscope. **Color version available online**.

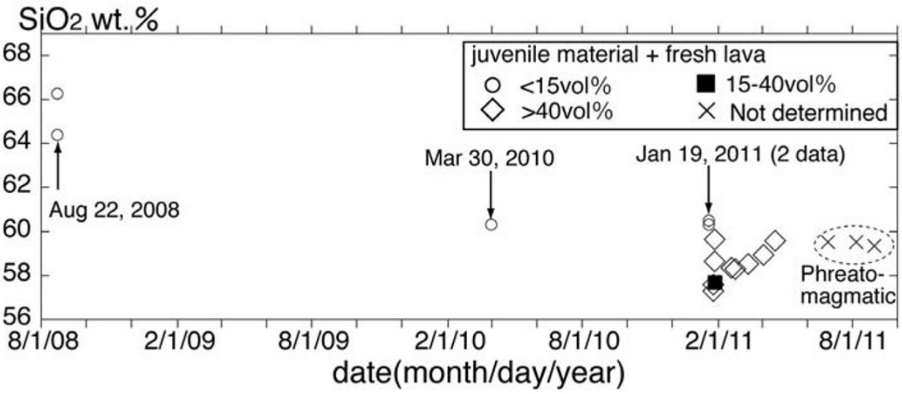


Fig. 11. Temporal change in bulk ash $SiO_2$ content. Different symbols indicate the total percentage (in number) of juvenile material and fresh lava in the analyzed sample (Fig. 2 and Table 2). See "second phreatomagmatic stage" in Subsection 5.1.2 for the reason why the total ratios could not be determined in and after June 2011.

compositions are plotted together with bulk rock compositions of 2011 rock samples (Suzuki *et al.*, 2013) and past ejecta (data originally reported in Tajima *et al.*, 2013, limited to data analyzed in ERI, as in the present ash study and Suzuki *et al.*, 2013). Figure 12 was made, because the ash samples can be mixtures of freshly erupted magma and fragments of past ejecta. An averaged $SiO_2$ content of 57–58 wt% is estimated for the erupted magma, as follows. Suzuki *et al.* (2013) showed that gray- and brown-colored pumice samples and lava samples in the 2011 eruption (57–58 wt% $SiO_2$; Fig. 12) are products of syneruptive mixing. White pumice blocks (62–63 wt% $SiO_2$), which are equivalent to the low-temperature endmember of the mixing, account for only several percent of pumice blocks in sub-Plinian phase (Suzuki *et al.*, 2013). 1716–1717 pumice data ($SiO_2$ = 57.2 wt%) shown in Fig. 12 matches the 1716–1717 gray pumice composition (57–58 wt%) determined by Miyamoto (2012), who comprehensively examined eight explosive eruption phases. Miyamoto (2012) also showed that gray pumice blocks are dominant relative to yellow (originally white) pumice blocks, as in the 2011 eruption. For the 1716–1717 lava and older ejecta, Tajima *et al.* (2013) showed that the majority has $SiO_2$ = 59–63, as plotted in Fig. 12.

In Fig. 12, most ash samples form linear trends (57.3–60.5 wt% $SiO_2$) within compositional ranges of most rock samples of Shinmoe-dake. In the $Na_2O$ and $K_2O$ diagrams, however, the high $SiO_2$ ends of the ash trends (59 wt% or more) depart from the compositional ranges of rock samples. The characteristics of ash samples as noted above are not applicable to August 2008 ash samples because; they have higher $SiO_2$ contents (64.4–66.3 wt%) than most of Shinmoe-dake rock samples, and they are not on linear trends formed by other ash and rock samples from present and past eruptions.

### 5.3 Particle size distribution

The size distribution data are shown in cumulative style in Fig. 13. There are systematic differences in the cumulative curves among the eruption stages, although each stage has variation. Data for the phreatic stage (2008 to 2010), the phreatomagmatic eruption (January 19, 2011) and the second phreatomagmatic stage (June to August 2011) resemble one another and are characterized by concave-upward curves. Sub-Plinian events and related eruptions (January 27–28, 2011), and the vulcanian stage (February and April 2011), are characterized by convex-upward curves. It is clear that the former group has smaller averaged particle sizes than the latter.

## 6. Discussion

### 6.1 Characteristics and temporal change of juvenile material

To confirm the identification of juvenile material based on its appearance under the microscope (as described in Subsection 5.1.1), Suzuki *et al.* (2013) determined compositions of phenocrysts in juvenile material ("fresh pumice" and "fresh scoria") and found them to resemble those of phenocrysts in 2011 lava and pumice blocks. But, analyses in Suzuki *et al.* (2013) were limited to ash samples with abundant juvenile material, and to abundant particle types (pumice particles on January 19 and scoria particles on February 18 and 24 and March 13, 2011). "Fresh pumice" and "fresh scoria" ash particles between August 2008 and June 2010 have not been analyzed. However, our conclusion that the eruption style for this period was phreatic will probably not be affected by future chemical analyses, because of 1) the lower abundance of juvenile material ($<1$ vol%) than in the following periods (Fig. 2, Table 2), and 2) the presence of a crater lake in this period (Fig. 14).

We next focus on other characteristics of the juvenile material that helped us define an eruptive stage. The pumice in the January 19, 2011 eruption has low vesicularity and a blocky or platy shape (Subsection 5.1.2, Figs. 5(a) and (c)). Such particle shapes can be formed when magma is quenched by external water (e.g. Suzuki and Nakada, 2002; Suzuki *et al.*, 2007). Pre-eruption investigation of the electrical resistivity structure beneath Shinmoe-dake revealed an aquifer at a depth of 100–1400 m (around sea level) below the summit (Kagiyama *et al.*, 1996). If the presence of a crater lake even after the January 19, 2011 eruption (Fig. 14) is considered, magma-water interaction during the January 19 event seems possible and even likely. We thus interpret the January 19 eruption to have been phreatomagmatic (Fig. 14).

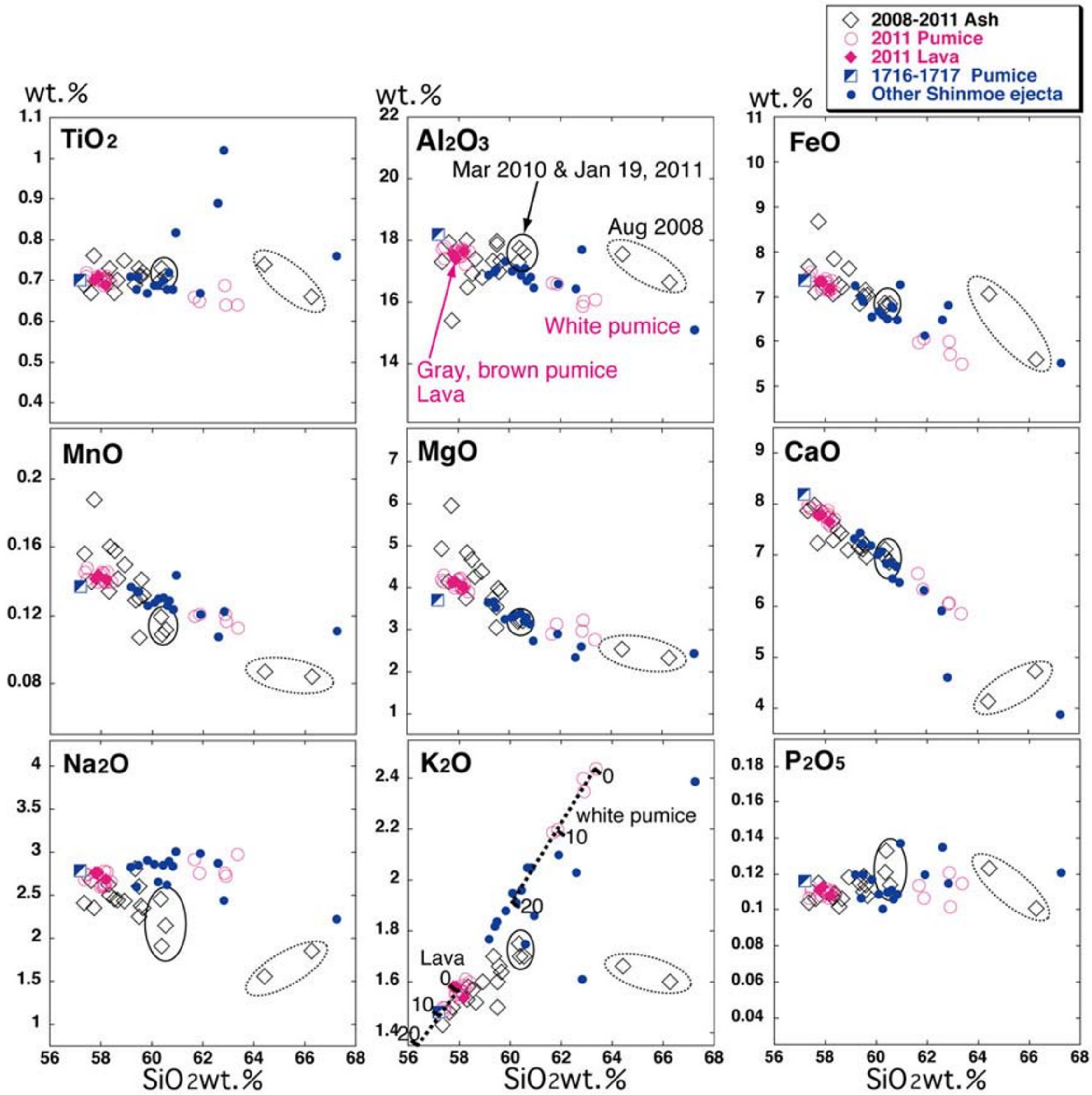


Fig. 12. $SiO_2$ variation diagrams for bulk ash compositions (2008–2011), and bulk rock compositions of Shinmoe-dake ejecta in 2011 eruption (Suzuki *et al*., 2013) and past eruptions (Tajima *et al*., 2013; blue plots). Compositions of ash erupted in early phase of 2010–2011 activity are enclosed by black ovals. For the 2011 eruption, data for pumice blocks (white, and gray- and brown-colored) are from the three sub-Plinian eruptions and later explosion (January 28), while lava data are from February 1 vulcanian eruption (Suzuki *et al*., 2013). Data for past ejecta excluding the 1716–1717 pumice include the Maeyama pumice (5.6 cal ka BP; Okuno, 2002) and lavas erupted in and prior to 1716–1717 eruption. For the 1716–1717 eruption, there is uncertainty about the timing of lava emplacement that took place after the explosive phases (Tajima *et al*., 2013). The lines with numbers (0, 10, 20) in the $SiO_2$-$K_2O$ diagram show the compositional changes of representative ejecta (2011 lava and white pumice), when up to 20 wt% of their groundmass (63.9 wt% $SiO_2$ and 2.4 wt% $K_2O$ in lava; 76.6 wt% $SiO_2$ and 4.5 wt% $K_2O$ in white pumice; Suzuki *et al*., 2013) is separated from the bulk rock composition. Also see Subsections 5.2 and 6.4. **Color version available online**.

### 6.2 Origin of "fresh lava" particles

Although "fresh lava" particles have a range of colors (e.g. Figs. 5(b), 6, 7(a)–(c), 8), they are consistent in their phenocryst assemblage and freshness relative to "partly altered" lava particles (accessory and accidental). We have not yet conducted detailed chemical analyses of "fresh lava" particles (e.g. phenocryst composition), but their petrographic features, including the phenocryst assemblage (olivine + two pyroxenes + plagioclase + Fe-Ti oxides), coincide with those of most of the 2011 ejecta, including lava ejected ballistically from the crater (Suzuki *et al*., 2013; most ejecta are products of syneruptive magma mixing). Accordingly, we judge that the "fresh lava" particles are either 1) dense parts of magma erupting at the time, or 2) fragments of lava that earlier accumulated in the crater (but only after its first appearance during the night of January 27, 2011; Section 2).

The "fresh lava" particles erupted between January 19 and January 27 are probably dense parts of erupting magma. Indeed, there are continuities in color and vesicularity between the juvenile material ("fresh pumice" and "fresh scoria") and the "fresh lava" for this period (Figs. 5(a)–(b) for January 19, 2011; Fig. 6 for the first sub-Plinian event). In more detail, the range in vesicularities of erupting magma could be due to processes such as 1) different degree of gas-phase separation from magma during syneruptive ascent, and 2) heterogeneity in magma-external water interaction, including variable quench depths and presence and

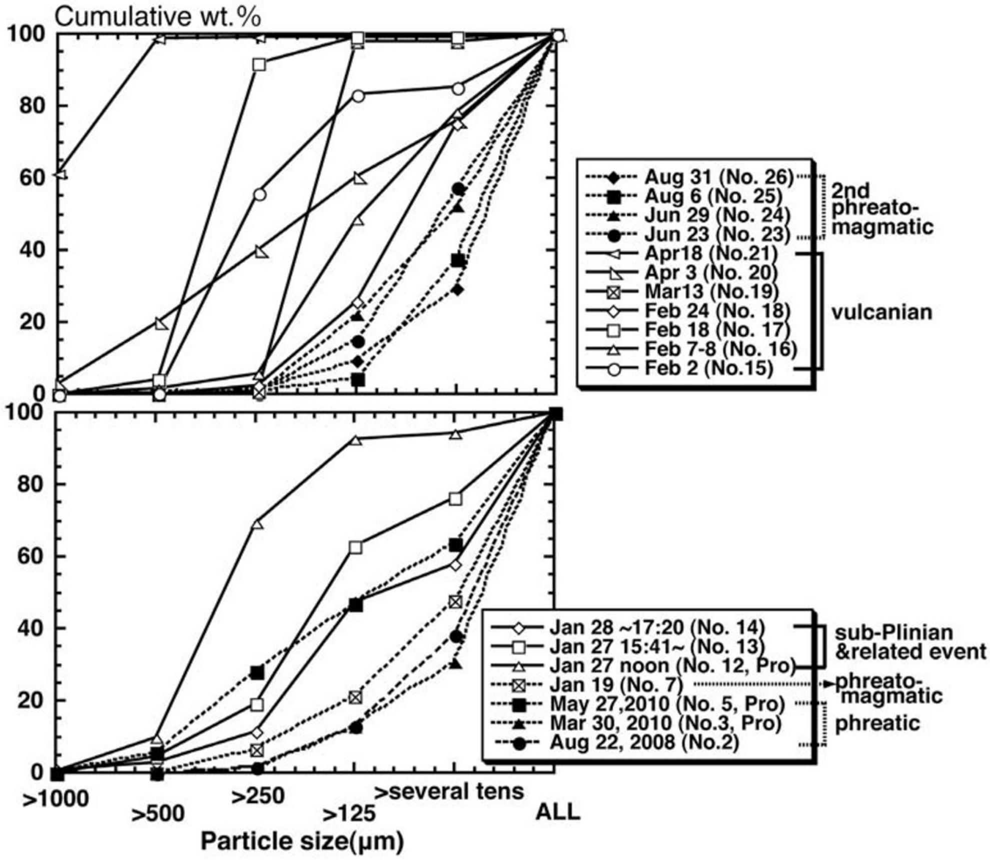


Fig. 13. Particle size distributions of ash samples. Dates of eruptions are shown without year if they occurred in 2011. No. indicates sampling site (Fig. 1 and Table 1) and "Pro" indicates sampling in proximal area (<3 km from the crater's center); all other samples are from 5 to 13 km distance. Note smaller average particle sizes in the phreatic stage and the two phreatomagmatic stages than in the other stages.

absence of a water quench, and 3) combination of 1) and 2) (Fig. 14). With regard to the January 19 eruption, co-ejection of pumice having water-quenching characteristics (6.1; Fig. 5(c)) indicates that "fresh lava" particles probably also resulted from magma-external water interaction.

The main products of the sub-Plinian stage are vesiculated pumice clasts (both ash particles and larger-size bombs). It is not known how the aquifer beneath the vent behaved during the sub-Plinian eruption, although crater water had disappeared by the completion of lava emplacement on the evening of January 29 (Section 2). Therefore, final judgment on whether external water was involved in the sub-Plinian stage requires future particle-surface textural studies using an SEM (e.g. Austin-Erickson *et al.*, 2008; Miyabuchi and Ikebe, 2008).

During the vulcanian stage, it is reasonable that most "fresh lava" particles were supplied from crater lava (Fig. 14), judging from the increased ratio of "fresh lava" particles relative to both "partly altered" lava particles and juvenile material ("fresh pumice" and "fresh scoria" particles) (Fig. 2, Subsection 5.1.2). The oxidation of some "fresh lava" particles (Fig. 7(c)) clearly indicates that they come from emplaced lava which was still hot at or near surface. We note that "fresh scoria" particles in this stage were also partly derived from unsolidified parts of crater lava, because "fresh scoria" particles are also oxidized (Fig. 9(a)).

### 6.3 Different phenocryst assemblages between lava particles and its effect on free-crystal assemblages

We found no olivine phenocryst in "partly-altered" lava particles (accessory material), in contrast to olivine-bearing "fresh lava" particles (Subsection 5.1.1). Recently, Tajima *et al.* (2013) reconsidered the whole eruptive history of Shinmoe-dake, based on 1) the stratigraphy in the crater-wall before the 2011 eruption, 2) re-categorization of both lava and tephra in other areas, and 3) new age determinations. Mafic phenocryst assemblages of lavas changed with time, from two pyroxenes in older lava flows to two pyroxenes + olivine in younger lava flows. We confirmed from thin sections that olivine phenocrysts in younger lava flows are only small microphenocrysts (<400 $\mu$m), whereas most of 2011 ejecta (magma-mixing products) have olivine phenocrysts as large as 1 mm (Suzuki *et al.*, 2013). Olivine microphenocrysts could be overlooked in thin sections of the partly altered lava particles and might be hard to see on the lava-particle surfaces under miscroscope, resulting in the original observation in 5.1.1.

"Free-crystals" in ash samples would have been derived not only from past lava but also from past pumice and scoria. Imura and Kobayashi (1991) and Tajima *et al.* (2013) showed that Setao pumice and Maeyama pumice, both erupted in the earliest phase of Shinmoe-dake activity (10.4 cal ka BP and 5.6 cal ka BP, respectively; Okuno, 2002), contain only two pyroxenes. Tajima *et al.* (2013)

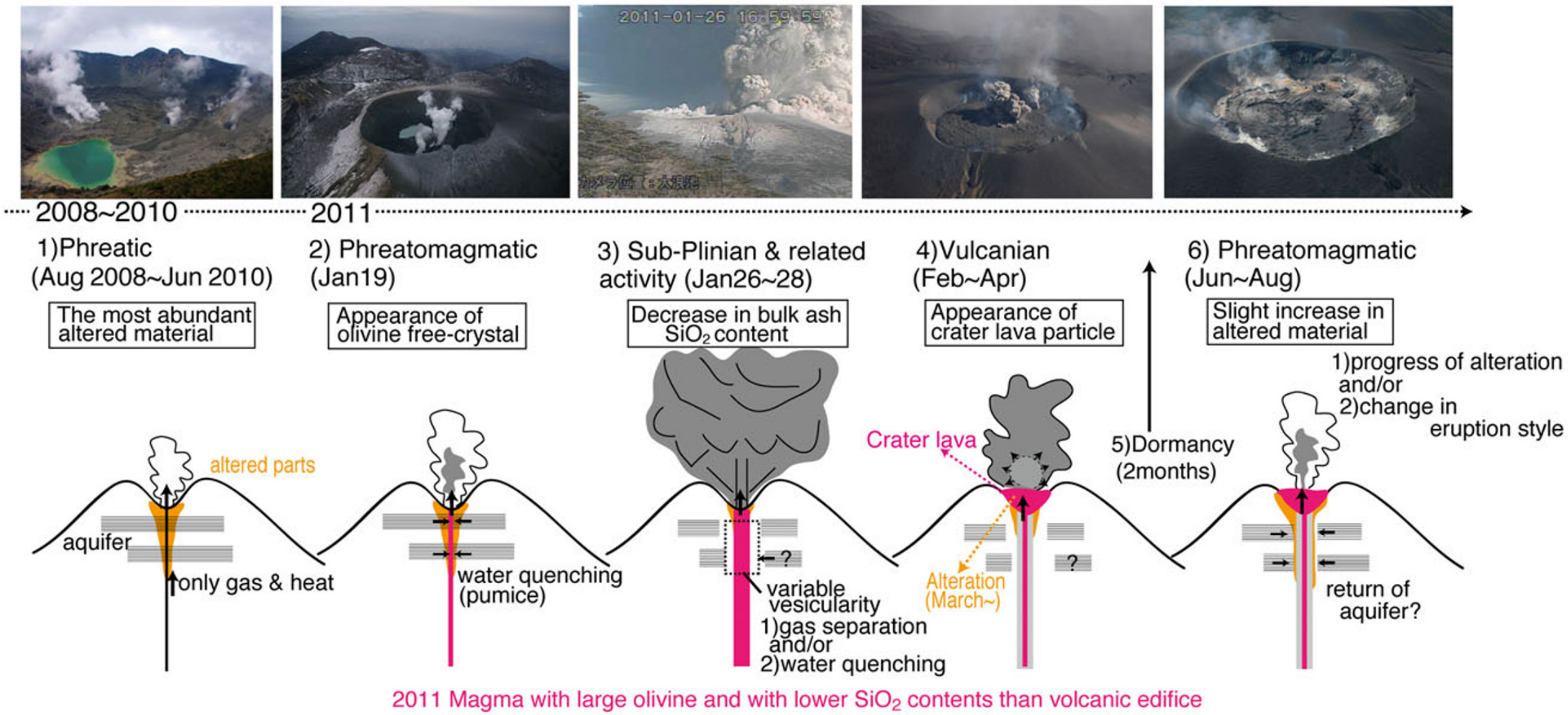


Fig. 14. Precursory phases and evolution of the 2011 eruption of Shinmoe-dake at Kirishima volcano, inferred from observation of ash samples. For detailed explanation, see related discussion and conclusion. The followings are dates and source of each photo; 1) phreatic (May 28, 2010; Bulletin on Volcanic Activity (May 2010) issued from Japan Meteorological Agency (JMA)), 2) phreatomagmatic (morning of January 21, 2011; courtesy of JMA), 3) sub-Plinian (January 26 17:00, 2011; Mt. Kirishima live camera located in Ohnami-ike), 4) vulcanian (February 4, 2011; T. Kaneko), 6) second phreatomagmatic period (August 13, 2011; courtesy of K. Shimousuki, Worth Planning Ltd.).

showed, for later-stage tephras excluding Kyoho Pumice (1716–1717), that mafic phenocryst assemblages change in a similar manner to those in lavas of similar age. For the Kyoho eruption (1716–1717), which consists of seven phases (Sm-KP1 to -KP7; Imura and Kobayashi, 1991), Miyamoto (2012) showed that pumice samples have the same phenocryst assemblage as do products of the 2011 eruption, but pumice samples with isolated olivine phenocrysts (i.e. free from a thick reaction rim) are limited to Sm-KP4 (200 $\mu$m in average olivine size). The above summary indicates that most pumices of past eruptions also lack large olivine phenocrysts. We thus conclude that the shift in free-crystal assemblage from olivine-free (2008 to 2010 eruptions) to olivine bearing (on and after January 19, 2011) resulted from input of 2011 magma bearing large olivine phenocrysts ($\sim$1000 $\mu$m) (Fig. 14).

### 6.4 Temporal change of bulk ash composition

The August 2008 ash samples have higher $SiO_2$ contents than do most of the 2011 rock samples (equivalent to erupted magma) and past ejecta (Fig. 12). This indicates that the 2008 samples are not simple mixtures of 2011 ejecta and past ejecta. The compositional variation of the 2010 and 2011 ash samples can be approximated by a mixture of the above two major ash constituents (Fig. 12). The ash components derived from the past ejecta are "partly altered pumice + scoria", "partly altered lava" and "altered material", while those derived from the erupted magma in 2011 are "juvenile material" and "fresh lava". Ash samples of post-January 19, 2011 eruptions have lower bulk $SiO_2$ contents than those of earlier eruptions (Fig. 11). Total ratios of "juvenile material" and "fresh lava" particles are higher in the post-January 19, 2011 eruptions (19.2–72.7 vol%), than in the earlier eruptions (0.4–12.6 vol%). The relationship can be explained by compositional differences between the erupted magma and past ejecta. As summarized in Subsection 5.2, the averaged composition of the erupted magma is 57–58 wt% $SiO_2$ (Suzuki *et al.*, 2013), whereas most past ejecta have 59–63 wt% $SiO_2$ (Tajima *et al.*, 2013) (Fig. 12). The contribution of 1716–1717 pumice fragments (57–58 wt% $SiO_2$; Miyamoto, 2012) to 2010 to 2011 ash samples seems small, because particle ratios of "partly altered scoria and pumice" are much lower than that of "partly altered lava" (Fig. 2). We thus conclude that the decrease in bulk ash $SiO_2$ content at the start of the sub-Plinian eruption (Fig. 11) was produced by an increased contribution of 2011 magma to the ash (Fig. 14). This model is consistent with the bulk ash compositions of March 2010 and January 19, 2011, which are comparable to the most frequent compositions of past ejecta (59–63 wt% $SiO_2$) excluding the 1716–1717 pumice (Fig. 12). We infer that the uncategorized "lava" particles in the second phreatomagmatic stage (June to August 2011; Subsection 5.1.2) consist of the same constituents as are in the vulcanian stage (i.e. "fresh lava" and "partly altered lava"), because of similar bulk ash compositions (Figs. 11 and 12) and similar juvenile material ratios (Fig. 2) between the two stages.

We infer that both the high $SiO_2$ contents of the 2008 ash samples and their deviation from the bulk trends of other ash samples (Fig. 12; Subsection 5.2) are due to the inclusion of abundant altered material (Fig. 2) in the analyzed bulk samples (Table 1). The silicification common in "altered material" (e.g. Fig. 3) would lead to an increase in $SiO_2$ content. The deviation of the 2008 ash from other bulk trends is most significant in $Na_2O$ and $K_2O$ (Fig. 12). A similar deviation was reported in the 2003 to 2004 eruption of Anatahan volcano; ash samples from its phreatomagmatic stage are depleted in alkali elements compared with rock samples of the volcano (Nakada *et al.*, 2005). Rock-fluid interaction may lead to alkali element depletion. Hamilton *et al.* (2000) showed that alkali elements have relatively high dissolution rates in glass that is immersed in a solution of high temperature and acidity. Ohba (2011) pointed out in his review that the existence of an acidic high temperature hydrothermal system is the most plausible condition that can produce altered mineral found in volcanic ejecta. At present, we are not certain how the rock-fluid interaction is related to the silicification process.

$Na_2O$ and $K_2O$ in the 2010–2011 ash samples deviate more from rock-sample trends at higher $SiO_2$ values (Fig. 12). Inclusion of silicified altered material may explain the deviation (e.g. March 2010 and January 19, 2011, and June to August, 2011; Fig. 2). To support this idea, we show that lowering the $K_2O$ trend by separation of $K_2O$-rich groundmass (i.e. groundmass separation model) is not possible (Fig. 12). The groundmass would be prone to be separated, because it can be fine particles due to syneruptive vesiculation. The two lines in the $SiO_2$ vs. $K_2O$ diagram (Fig. 12) show trends that can be formed by different degrees of groundmass separation from representative erupted magma (2011 lava and white pumice). The two trends remain parallel to the original whole rock trends of other ejecta; therefore, the groundmass separation model can be rejected.

### 6.5 Variation of particle size distribution

The grain size distribution of ejecta just after discharge from the crater reflects syn-eruptive fragmentation conditions. Accordingly, the size distribution helps us judge the eruption style, including possible involvement of external water (Morrissey *et al.*, 2000). However, interpretation of samples collected at a distance from the crater requires careful considerations of the sorting process, which is influenced by plume height, distance from crater and dispersal axis, and meteorological conditions. To evaluate possible differences in particle size distribution at the time of ejection, we here take both plume height and distance from crater into consideration. At first place, most sampling distances from the center of the crater are similar, except for the phreatic stage (August 2008 to June 2010) (sites 3, 4, 5, and 6 in Fig. 1). The samples, excluding the phreatic stage, have differences in average particle size, coarser in the sub-Plinian and vulcanian stages and finer in the two phreatomagmatic stages (Fig. 13). The difference may have been influenced by different eruption plume heights; heights of $>$1000 m characterize the sub-Plinian and vulcanian stages, while heights mostly $<$1000 m typify other stages (Table 1).

In the phreatic stage (August 2008 to June 2010), ash samples are generally fine regardless of the sampling sites, including sites 3 and 5 close to the crater (Pro in Fig. 13), indicating the overall fineness and thereby implying involvement of external water. This inference is consistent with the presence of a crater lake at this stage (Fig. 14) and the occurrence of a cock's tail explosive jet during the May 27, 2011 eruption (Bulletin on Volcanic Activity (May 2010) issued from JMA).

For the January 19, 2011 eruption, we have information about neither grain-size variation with distance from crater nor the conditions of the crater at the time of eruption. The particle size data for this event are only from one place (site 7; Fig. 1). But, the presence of juvenile pumice with water-quenched texture (Subsection 6.1) indicates involvement of external water. Therefore, we believe that the fine grain size of the ash in this eruption (Fig. 13) also resulted from the interaction with external water. JMA reported that a small crater lake existed just after the eruption (Fig. 14).

In the second phreatomagmatic stage (June to August 2011), no sample was collected from proximal sites (<3 km from the crater center; Fig. 13). The ash is probably fine regardless of distance from the crater, however, to judge from the 5-km sample (August 6, 2011; site 25 in Fig. 13) and the 6–7-km samples (sites 23, 24, 26 in Fig. 13). Phreatomagmatic eruptions are seen to continue longer than other eruptions (Nakada *et al.*, 2013), and eruptions in this stage lasted longer (e.g. June 29 to July 1 and August 31 to September 6; Table 1) than those during the vulcanian stage. The evidence thus suggests that the fine grain size of the ash resulted from interaction of magma with external water (Fig. 14). Vesicularities of juvenile particles in this stage seem relatively high (Fig. 10), but vesicularity during magma-water interaction could vary depending on the degree of gas-phase separation from magma before the time of the interaction.

The ash samples from the second phreatomagmatic stage (June to August 2011) have larger amounts of altered material than do samples from the vulcanian stage (Fig. 2). At present, we infer that the increase is related to either 1) progressive alteration in the conduit-crater system due to supply of fluid from intruded magma (Fig. 14), or 2) change of eruption style. We deny effect of changing vent locations, as they were almost the same as previous vulcanian stage (e.g. Nakada *et al.*, 2013). Progressive alteration is supported by the crater photo (Fig. 14) and direct observation of lava particles in ash (Subsection 5.1.2 and Fig. 8). To further test our interpretation of magma-water interaction in the first phreatomagmatic stage (January 19, 2011) and the second phreatomagmatic stage (June to August, 2011), future study should focus on detailed observations of particle surface texture with an SEM (e.g. Austin-Erickson *et al.*, 2008; Miyabuchi and Ikebe, 2008).

### 6.6 Successful detection of juvenile material before the January 26, 2011 sub-Plinian eruption and task for future studies

Since the August 2008 eruption, researchers at the volcano research center of ERI (Y.S. and F.M.) have been making ash-sample reports for every eruption, in response to requests from JMA. Experience and knowledge acquired from these precursory events helped Y.S. to find juvenile material (pumice; Fig. 5) quickly, just after receiving the January 19, 2011 ash samples from JMA. Regrettably, the time between sending a report to JMA (noon of January 26) and the start of the first sub-Plinian event was too short to inform all of Japan's volcanologists that magma had risen to shallow depth. But, as far as we know, ash characterization was the only method which detected the change of eruptive activity before the sub-Plinian event itself. Although ash samples cannot predict the scale of an eruption, we again emphasize the importance of continuous ash sample observation starting from a period of low activity. We also note the necessity of one-by-one ash particle examination—time-consuming work—for the correct characterization of ash samples and early detection of juvenile material.

As a task for future eruptions, we here note difficulty of juvenile material identification in continuous eruptive activity (e.g. vulcanian stage in the 2011 eruption). The difficulty arises from that ash erupted in later stage of a continuous eruptive activity can include juvenile particles that once deposited inside the crater, i.e. recycled particles. If long-term dormancy takes place, the deposit inside the crater would be altered, resulting in an ease of juvenile material identification in next magmatic eruption (e.g. the first and second phreatomagmatic stages in the 2011 eruption). For more sophisticated identification of juvenile material, introduction of another objective indexes is preferable.

## 7. Conclusion

We studied a series of ash samples from the 2011 Shinmoe-dake eruption and its precursory eruptions in 2008 to 2010 to 1) define eruption stages, including information on magma-water interaction, and 2) infer changes in the volcanic edifice as eruptive activity progressed (Fig. 14). The 2011 eruption followed a course of a phreatomagmatic stage (January 19), a sub-Plinian and lava accumulation stage (end of January), a vulcanian stage (February–April), and second phreatomagmatic stage (June–August).

1) Judging from the smaller amount of fresh pumice and scoria (<1 vol%) than in the following stages, eruptions between August 2008 and June 2010 can be defined as phreatic. The fine ash samples also support the involvement of external water in the eruptions. The amount of altered material is the highest through the whole activity, probably because altered parts of the volcanic edifice were destroyed by the early eruptions.

2) The January 19, 2011 eruption can be classed as phreatomagmatic, based on a) the obvious appearance of juvenile material (8 vol% pumice) with water-quench textures, and b) the fineness of the ash. The presence of the juvenile material was reported to JMA before the start of the sub-Plinian event.

3) On January 26–28, 2011, the amount of juvenile scoria and pumice changed according to eruption intensity, reaching a maximum (50 vol%) in sub-Plinian events. The origin of fresh lava particles having continuities of color and vesicularity between the juvenile particles is not solved (probably either relativley dense parts of the erupted magma or water-quench products).

4) After lava accumulated in the crater at the end of January 2011, the particles from the lava accounted for 30–70 vol% of ash samples.

5) In the vulcanian stage, the total content of juvenile pumice and scoria first increased and then decreased over

a range of <15 vol%. The amount correlates weakly with eruption plume height.

6) We tentatively defined a period between June and August, 2011 as a second phreatomagmatic stage, based on finer ash and longer eruptive events than in the vulcanian stage. Juvenile pumice and scoria particles were still as abundant as during the vulcanian stage. The ratio of altered material is higher than in the vulcanian stage, because of progressive alteration of the volcanic edifice or a change in eruption style.

7) Bulk ash $SiO_2$ contents are lower in post-January 19, 2011 eruptions. The systematic change was caused by the higher average $SiO_2$ content of past ejecta than that of the 2011 erupted magma. An exception is that bulk ash compositions of the August 2008 ash samples were influenced by abundant altered material.

8) The free-crystal assemblages of ash samples are two pyroxenes + plagioclase + Fe-Ti oxides until 2010; olivine joins the assemblage in the January 19, 2011 eruption. Different assemblages and sizes of phenocrysts between the past ejecta (derived from the volcanic edifice) and the 2011 magma caused this change.

**Acknowledgments.** We are indebted to Japan Meteorological Agency for supplying us with ash samples and information on eruptive activity. Dr. K. Aizawa, Dr. J. Hirabayashi, Dr. R. Imura, Kirishima Geopark, Dr. T. Kobayashi, Mr. M. Sakagami, Dr. H. Sato, Mr. Y. Tajima, Takaharu-cho, Dr. M. Ukawa (in alphabetical order) are thanked for the ash samples. Also, Mr. Y. Tajima kindly taught us the eruptive history of Shinmoe-dake and petrographical and geochemical characteristics of past ejecta. Dr. T. Miyamoto kindly taught us petrographical and geochemical characteristics of 1716–1717 pumice samples. We express our thanks to members of the volcano research center of Earthquake Research Institute for discussions and assistance throughout this research. Finally, the manuscript was greatly improved by insightful comments from Dr. Donald Swanson (USGS), Dr. Jacopo Taddeucci (The Istituto Nazionale di Geofisica e Vulcanologia) and Dr. Thomas Wright (Johns Hopkins University). Also, they kindly improved the English manuscript. This work was partly supported by Grant-in-Aid from MEXT to S. Nakada (No. 22900001).

## References

Ando, S., The geomorphic change of the summit crater and the ground deformation around Shinmoe-dake, Kirishima volcano, revealed by ALOS data, *Rep. Coord. Comm. Predict. Volcan. Erup.*, **109**, 179–191, 2012 (in Japanese).

Austin-Erickson, A., R. Büttner, P. Dellino, M. H. Ort, and B. Zimanowski, Phreatomagmatic explosions of rhyolitic magma: Experimental and field evidence, *J. Geophys. Res.*, **113**, B11201, doi:10.1029/2008JB005731, 2008.

GIAJ (Geospatial Information Authority of Japan), Crustal deformations around Kirishima Volcano, *Rep. Coord. Comm. Predict. Volcan. Erup.*, **108**, 197–220, 2012 (in Japanese).

Hamilton, J. P., C. G. Pantano, and S. L. Brantley, Dissolution of albite glass and crystal, *Geochim. Cosmochim. Acta*, **64**, 2603–2615, 2000.

Hatae, K., K. Watanabe, K. Watanabe, T. Tsutsui, and Y. Motomura, Variation in content of vesiculated glasses in volcanic ash errupted from Kuju Volcano in 1995–96, Japan, *Bull. Volcanol. Soc. Jpn.*, **42**, 345–353, 1997 (in Japanese with English abstract).

Ichihara, M., M. Takeo, A. Yokoo, J. Oikawa, and T. Ohminato, Monitoring volcanic activity using correlation patterns between infrasound and ground motion, *Geophys. Res. Lett.*, **39**, L04304, doi:10.1029/2011GL050542, 2012.

Ikebe, S., K. Watanabe, and Y. Miyabuchi, The sequence and style of the 1988–1995 eruptions of Nakadake Aso Volcano, Kyushu, Japan, *Bull. Volcanol. Soc. Jpn.*, **53**, 15–33, 2008 (in Japanese with English abstract).

Imura, R. and T. Kobayashi, Eruptions of Shinmoedake Volcano, Kirishima Volcano Group, in the last 300 year, *Bull. Volcanol. Soc. Jpn.*, **36**, 135–148, 1991 (in Japanese with English abstract).

Kagiyama, T., H. Utada, M. Uyeshima, F. Masutani, W. Kanda, Y. Tanaka, H. Masuda, H. Murakami, I. Shiozaki, M. Ichiki, T. Yukutake, T. Mogi, K. Amita, N. Oshiman, and M. Mishima, Resistivity structure of the central and the southeastern part of Kirishima volcanoes, *Bull. Volcanol. Soc. Jpn.*, **41**, 215–225, 1996 (in Japanese with English abstract).

Kozono, T., H. Ueda, T. Ozawa, T. Koyaguchi, E. Fujita, A. Tomiya, and Y. J. Suzuki, Magma discharge variations during the 2011 eruptions of Shinmoe-dake volcano, Japan, revealed by geodetic and satellite observations, *Bull. Volcanol.*, **75**, 695, 2013.

Maeno, F., M. Nagai, S. Nakada, R. Burden, S. Engwell, Y. Suzuki, and T. Kaneko, Constraining tephra dispersion and deposition from cyclic subplinian explosions at Shinmoedake volcano, Kyushu, Japan, *Japan Geoscience Union Meeting 2012*, SVC50-07, 2012.

Maeno, F., S. Nakada, M. Nagai, and T. Kozono, Ballistic ejecta and eruption condition of the vulcanian explosion of Shinmoedake volcano, Kyushu, Japan on 1 February, 2011, *Earth Planets Space*, **65**, this issue, 609–621, doi:10.5047/eps.2013.03.004, 2013.

Miyabuchi, Y. and S. Ikebe, The February 2008 ash deposit from the Nakadake crater, Aso volcano, Japan, *Bull. Volcanol. Soc. Jpn.*, **53**, 201–206, 2008 (in Japanese with English abstract).

Miyabuchi, Y., S. Ikebe, and K.Watanabe, Geological constraints on the 2003–2005 ash emissions from the Nakadake crater lake, Aso Volcano, Japan, *J. Volcanol. Geotherm. Res.*, **178**, 169–183, 2008.

Miyagi, I., J. Itoh, H. Shinohara, and Kagoshima Observatory, Japan meteorological agency, re-activation process of Showa volcanic vent at Sakurajima volcano in 2008: Evidence from volcanic ash. Japan, *Bull. Volcanol. Soc. Jpn.*, **55**, 21–39, 2010 (in Japanese with English abstract).

Miyamoto, T., Magma systems of the Kyoho eruption in Shinmoe-dake volcano, Kirishima volcanoes: 2, *Japan Geoscience Union Meeting 2012*, SVC50-P43, 2012.

Morrissey, M., B. Zimanowski, K. Wohletz, and R. Buettner, Phreatomagmatic fragmentation, in *Encyclopedia of Volcanoes*, edited by H. Sigurdsson, 431–445, Academic Press, New York, 2000.

Nakada, S., Y. Motomura, and H. Shimizu, Manner of magma ascent at Unzen Volcano (Japan), *Geophys. Res. Lett.*, **22**, 567–570, 1995.

Nakada, S., T. Matsushima, M. Yoshimoto, T. Sugimoto, T. Kato, T. Watanabe, R. Chong, and J. T. Camacho, Geological aspects of the 2003–2004 eruption of Anatahan Volcano, Northern Mariana Islands, *J. Volcanol. Geotherm. Res.*, **146**, 226–240, 2005.

Nakada, S., M. Nagai, T. Kaneko, Y. Suzuki, and F. Maeno, The outline of the 2011 eruption at Shinmoe-dake (Kirishima), Japan, *Earth Planets Space*, **65**, this issue, 475–488, doi:10.5047/eps.2013.03.016, 2013.

Nakao, S., Y. Morita, H. Yakiwara, J. Oikawa, H. Ueda, H. Takahashi, Y. Ohta, T. Matsushima, and M. Iguchi, Volume change of the magma reservoir relating to the 2011 Kirishima Shinmoe-dake eruption—Charging, discharging and recharging process inferred from GPS measurements, *Earth Planets Space*, **65**, this issue, 505–515, doi:10.5047/eps.2013.05.017, 2013.

Ohba, T., Hydrothermal mineral-bearing volcanic products: Relationships with subvolcanic hydrothermal systems, and styles and patterns of their formation, *J. Geol. Soc. Jpn.*, **117**, 344–356, 2011 (in Japanese with English abstract).

Ohba, T. and Y. Kitade, Subvolcanic hydrothermal systems: Implications from hydrothermal minerals in hydrovolcanic ash, *J. Volcanol. Geotherm. Res.*, **145**, 249–262, 2005.

Oikawa, J., A. Watanabe, H. Tsuji, Y. Morita, T. Koyama, T. Ohminato, M. Takeo, S. Nakada, Y. Aoki, and M. Ichihara, Volcanic earthquakes and tremor associated with the 2008–2011 Shinmoe-dake eruption, *Fall Meeting of the Volcanological Society of Japan*, A1-11, 2011 (in Japanese).

Okuno, M., Chronology of tephra layers in Southern Kyushu, SW Japan, for the last 30,000 years, *Quatern. Res.*, **41**, 225–236, 2002 (in Japanese with English abstract).

Ozawa, T. and T. Kozono, Temporal variation of the Shinmoe-dake crater in the 2011 eruption revealed by spaceborne SAR observations, *Earth Planets Space*, **65**, this issue, 527–537, doi:10.5047/eps.2013.05.004, 2013.

Rowe, M. C., C. R. Thornber, and A. J. R. Kent, Identification and evolution of the juvenile component in 2004–2005 Mount St. Helens ash, in *A Volcano Rekindled: The Renewed Eruption of Mount St. Helens, 2004–2006*, edited by D. R. Sherrod, W. E. Scott, and P. H. Stauffer, U.S. Geological Survey Professional Paper 1750, 335–382, 2008.

Sasaki, H., K. Isobe, S. Homma, M. Sakagami, S. Mukoyama, S. Nakada, T. Kobayashi, and M. Murakami, Estimation of lava volume using oblique aerial photo in Shinmoedake Volcano, *Fall Meeting of the Volcanological Society of Japan*, A1-13, 2011 (in Japanese).

Shimano, T., S. Nakada, and T. Kaneko, Evaluation of magmatic contribution to the 2000 eruption at Usu Volcano, North Japan, by XRF bulk ash composition analysis, *Bull. Earthq. Res. Inst.*, **76**, 247–251, 2001 (in Japanese with English abstract).

Shimbori, T. and K. Fukui, Time variation of the eruption cloud echo height from Shinmoe-dake volcano in 2011 observed by Tanegashima and Fukuoka weather radars, *Rep. Coord. Comm. Predict. Volcan. Erup.*, **108**, 189–196, 2012 (in Japanese).

Suzuki, Y. and S. Nakada, Vesiculation and magma ascent process in the Usu 2000 eruption, inferred from texture and size distribution of bubbles, *Bull. Volcanol. Soc. Jpn.*, **47**, 675–688, 2002 (in Japanese with English abstract).

Suzuki, Y., J. E. Gardner, and J. F. Larsen, Experimental constraints on syneruptive magma ascent related to the phreatomagmatic phase of the 2000AD eruption of Usu volcano, Japan, *Bull. Volcanol.*, **69**, 423–444, 2007.

Suzuki, Y., A. Yasuda, N. Hokanishi, T. Kaneko, S. Nakada, and T. Fujii, Syneruptive deep magma transfer and shallow magma remobilization during the 2011 eruption of Shinmoe-dake, Japan—Constraints from melt inclusions and phase equilibria experiments—, *J. Volcanol. Geotherm. Res.*, **257**, 184–204, 2013.

Taddeucci, J., M. Pompilio, and P. Scarlato, Monitoring the explosive activity of the July–August 2001 eruption of Mt. Etna (Italy) by ash characterization, *Geophys. Res. Lett.*, **29**, doi:10.1029/2001GL014372, 2002.

Taddeucci, J., M. Pompilio, and P. Scarlato, Conduit processes during the July–August 2001 explosive activity of Mt. Etna (Italy): inferences from glass chemistry and crystal size distribution of ash particles, *J. Volcanol. Geotherm. Res.*, **137**, 33–54, 2004.

Tajima, Y., S. Hayashi, A. Yasuda, and H. Itho, Tephrostratigraphy and eruptive history of Shinmoedake volcano of the Kirishima volcanoes, Kyushu, Japan, *Quatern. Res.*, **52**, 2013 (in Japanese with English abstract).

Tsutsui, M., K. Tomita, and T. Kobayashi, Fumarolic activity since December 2003 and volcanic activity during the Meiji and Taisho Eras (1880–1923) of Ohachi Volcano, Kirishima Volcano Group, Southern Kyushu, Japan, *Bull. Volcanol. Soc. Jpn.*, **50**, 475–489, 2005 (in Japanese with English abstract).

Ueda, H., T. Kozono, E. Fujita, Y. Kohno, M. Nagai, Y. Miyagi, and T. Tanada, Crustal deformation associated with the 2011 Shinmoe-dake eruption as observed by tiltmeters and GPS, *Earth Planets Space*, **65**, this issue, 517–525, doi:10.5047/eps.2013.03.001, 2013.

Yakiwara, H., K. Goto, S. Hirano, H. Miyamachi, and S. Nakao, Seismicity in and around Kirishima Volcanic Group for recent 10 years and temporary seismic observation, *Japan Geoscience Union Meeting 2011*, SVC070-P42, 2011.

---

Y. Suzuki (e-mail: ysuzuki@eri.u-tokyo.ac.jp), M. Nagai, F. Maeno, A. Yasuda, N. Hokanishi, T. Shimano, M. Ichihara, T. Kaneko, and S. Nakada